Available online www.jsaer.com

***Journal of Scientific and Engineering Research*, 2023, 10(3):47-62**

Research Article

ISSN: 2394-2630
CODEN(USA): JSERBR

Finite element modeling of flexible pavement structures: study of parameters related to tire configuration

Babacar Diouf[1], Makhaly Ba[1], Bibalo Ida Josiane KI[1]

[1]Laboratory of Mechanics and Modeling (L2M), Faculty of Engineering Sciences, Iba Der Thiam University of Thiès, Thiès, Sénégal.
e-mail: babacar.diouf82@univ-thies.sn

Abstract In the design of pavement structures in Senegal, heavy vehicle traffic is an essential factor. Their rapid evolution considerably modifies the load distribution in the pavement structure. With three-dimensional modeling and in order to simulate the loading faithfully, the application of the wheel contact area is described by two discs of radium 0.125 m and center-to-center spacing of 0.375 m. In the mechanistic method of design, the axle load is assumed to be uniformly distributed over the contact area. In order to study the effect of the dual wheels, a vertical contact stress distribution is studied to evaluate the maximum strain on the space described by the dual wheels. The results showed that the vertical strain is maximum at the center of the circular surface. It is also generally found that the stresses and strains created by the single wheel is greatest at the surface of the wearing course. However, at a certain depth of this layer, there is a reversal, that is to say the strains and stresses created by the dual wheel is greater up to the base of the base layer. It can be seen that this difference decreases very quickly in the sub-base layer and even tends to cancel out in some cases down to the subgrade. The pavement structure considered is made up of a Diack basalt base course and a Sindia laterite sub-base course. The wearing course is made of bituminous concrete and the whole rests on a support subgrade. The behavior of the base and sub-base layer will be considered nonlinear while the behavior of the wearing course and subgrade is linear. Within the framework of this finite element modeling of a flexible pavement structure, two loading cases are studied, that of a single wheel and a dual wheel.

Keywords Modeling, finite element, flexible pavement, laterite, basalt, loading, wheels, nonlinear, behavior

Introduction

The design of pavement structures is becoming more and more complex because they are subjected to increasingly high mechanical stresses, but also to environmental factors. Heavy vehicles represent the most aggressive elements of traffic in terms of stresses. The rapid evolution of their configuration has the consequence of significantly modifying the load transfer on the pavement surface.

Traffic loads are applied to the pavement by tires that exert forces on the tire-pavement contact surface. In Senegal, the reference load taken into account is that of 130 kN consisting of two duals wheels. The loading considered in the simulation is that of a 130 kN dual wheel half axle and a 65 kN single wheel in order to evaluate the impact of the axle configuration on the pavements. The loading is distributed and applied to one and two finely meshed footprints located on the surface layer. However, the domain size configuration of the pavement structure, traffic load simulation and mesh refinement are the most important factors [1].

For the design, the load transfer on the pavement surface depends on the characteristics of the load adopted. The load adopted for the design is a static load distributed over two 0.125 m radius disks with and interaxis of 0.375 m. Pavement analysis and design methods generally assume a uniform load distribution over a circular surface. However, pavement loading created by traffic is summarized as repeated and cyclic loading on the pavement

surface. These can be broken down into vertical (vehicle weight) and horizontal (acceleration and braking) loads [2]. This traffic loading cases will be studied, that of a single wheel and a dual wheel.

Finite element modeling of pavement structures

The finite element approach provides the best method for analyzing multi-layered pavement systems [3]. Two-dimensional, three-dimensional, or axisymmetric finite element models have different formulations and consider different stress and strain components. Compared to the multilayer elastic method, the finite element method is better because it can rigorously account for anisotropy, material nonlinearity, and various boundary conditions [4].

However, these two-dimensional models have limitations. They cannot take into account not uniform tire contact pressures and multiple rolling loads. To overcome these limitations, three-dimensional finite element approaches are becoming increasingly popular. With 3D analyses, the responses of flexible pavements are studied under spatially varying tire contact pressures, it is also possible to capture the effect of material nonlinearity as well as the effect of the finite element approach can be difficult and often takes more time.

Finite element modeling for solving linear or nonlinear structural problems can be done in three phases.

- Preprocessor phase: this step consists in defining the mathematical model representative of the physical model of the structure, specifying the calculation options (2D, 3D, etc.), the discretization of the different parts of the structure (nodes, types of elements, etc.), the mechanical models to be associated with the mesh (boundary conditions, loading, etc.);
- Calculation phase: resolution of the discretized problem (calculation and assembly of the elementary stiffness matrices, resolution of the linear or nonlinear system, etc.);
- Post-processor phase: analysis and processing of results (displacements, stresses, strain, etc.).

In the following, we will use the finite element code CAST3M which is a modeling program widely applied to the analysis of road pavements.

CAST3M is a software package for calculating structures using the finite element method and more generally for solving partial differential equations using the finite element method. It was developed at the Department of Mechanics and Technology (DMT) of the French Atomic Energy Commission (CEA).

The main characteristic of CAST3M is to be extremely adaptable to the multiple applications specific to each user. The development of CAST3M is part of a research activity in the field of mechanics whose object is to define a high level tool, which can be used as a support for the design, dimensioning and analysis of structures and components, in the nuclear field as well as in the classical industrial sector. In this perspective, CAST3M integrates not only the calculation processes themselves but also the model building functions (pre-processor) and the results processing functions (post-processing). CAST3M is a program that the user can adapt to his needs to solve his own problems.

CAST3M has a command language consisting of a series of operators allowing the user to manipulate data and results in the form of objects by giving them names: this is the Gibiane language using a text editor (any one). Then launch the CAST3M application on the created file.

Solving mechanical problems requires the knowledge of boundary conditions, loading condition and the behavioral law that relates strains to stresses. Most commercial finite element software offers, in addition to a large choice of behavioral laws, the possibility to implement one's own law when no model in the provided library is able to adequately represent the behavior of the material used. This alternative is offered with the CAST3M software.

Effect of axle configuration

The mechanical stresses taken into account in the design of pavements come from traffic loads. These loads are applied to the pavements through the intermediary of the tires which exert forces on the contact surface. These tires can be either single or dual wheels (figure 1). [5] reported that the stresses and strains caused depends not only on the weight of the vehicle, but also on the configuration of the axles (single, tandem, tridem). Increasing the number of axles reduces the load transmitted to the pavement surface [6]. Indeed, a single axle produces more strains than a tandem axle [1]. Similarly, a tridem axle produces less strain than a tandem axle. [7] point out that there is a very large difference between the various wheel types. They argue that single wheels cause more strains because of the increased contact pressures they generate. [8] [9] confirm this, indicating that this stresses and strains are related to tire width and contact pressure. The work of [10] on the response of various

types of flexible pavements shows that the strains obtained under single wheel loading are much greater than the strains obtained under dual wheel loading.

a) b)

Figure 1: Axle configuration [8]: a) single wheel b) dual wheel

Mechanical characteristics of materials

The materials used in the pavement base courses in this study are untreated gravel from the Diack (basalt) and Sindia (laterite) quarries. These quarries are all located in Senegal. These materials were previously tested at the Laboraty of Mechanics and Modeling (L2M) of the Engineering Sciences Department of the Iba Der Thiam University of Thiès, at the Cheikh Anta Diop University of Dakar, at the University of Paris-Est, and at the University of Wisconsin in the United States of America.

Diack basalt was widely used as a surface course for bituminous pavement. However, with the increase in traffic volume and axle loads, Diack basalt is increasingly used as a base or sub-base layer for flexible pavements. It is often used in the form of untreated gravel 0/31,5 often in the form of Grave bitumen 0/20 with high performances. This material is well known and constitutes a good reference material in Senegal [11].

As for laterite, it still constitutes the bulk of the road network in Senegal. The plasticity of this material varies widely, from one deposit to another, and even within the same deposit. Often, laterites are so plastic that they can only be used as pavement material after stabilization [3].

Recent studies by [12] show that Sindia laterite meets the requirements of [13] for use as a sub-base. Atterberg limit tests conducted by [14] confirm those of [12]. Their results reveal that Sindia laterite falls within the Casagrande diagram in the medium plasticity range. In table 1, the parameters of the Atterberg limits and those of the modified Proctor parameters of the laterite of Sindia are summarized.

Table 1: Atterberg and modified Proctor limit parameters of Sindia laterite

Modified Atterberg and Proctor limit parameters	**Laterite of Sindia**	**CEBTP specifications (1984)**
Optimal density g/cm^3	1,97	$\geq 1,9$
Liquidity limit W_l (%)	29,85	≤ 50
Plasticity index I_p (%)	9,2	≤ 25

Grain size analysis (Standard NF P 94-056: 1996) and sedimentometry (Standard NF P 94-057: 1992) were performed on these two materials (Diack basalt and Sindia laterite) (figure 1) and the particle size characteristics are summarized in the table 2. The particle size curves of the materials fit well into the specification spindles defined by [3], as in Senegal, materials are often selected by reference to CEBTP rules [14]. The values of the uniformity coefficients $C_u \geq 2$ prove that the grading curves are all spread out and therefore the materials have the advantage of high densities, low permeabilities and are easily compacted [15].

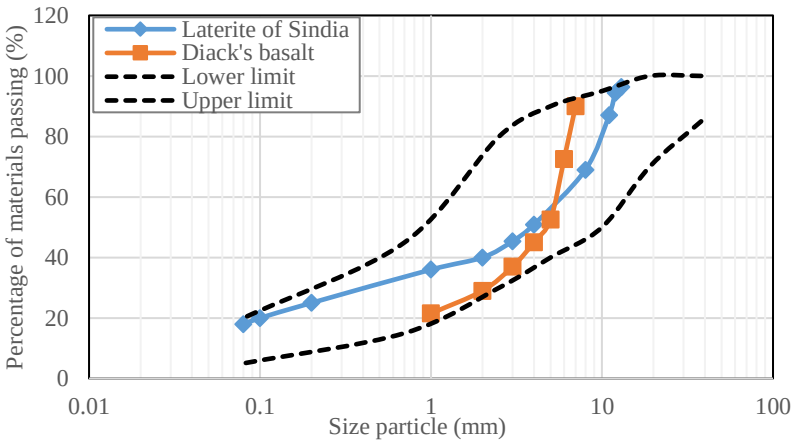

Figure 2: Particle size distribution of Diack basalt and Sindia laterite

Table 2: Particle size characteristics of materials

	Granulometric characteristics			
Material	C_c	C_u	**% fine**	$< 2\ mm$
Diack's basalt	3.84	66	8	18
Laterite of Sindia	0.34	207	17.86	41.6

Compaction is carried out at 95% of the Modified Optimum Proctor (OPM) which corresponds to the CEBTP road specifications for untreated gravel base courses in Senegal.

The compaction ability of untreated gravel is evaluated from the modified Proctor test, according to the French standard (NF P 94-093: 1993). On table 3, are represented the compaction and bearing capacity parameters of basalt and laterite materials. [11], based on his work, finds that Diack basalt has a high dry density compared to Bakel sandstones and Bandia and Bargny limestones. This low volume weight of limestones compared to basalt is noted by [16] as well. This slight difference noted between the work of the two researchers would be explained on the one hand to the difference in percentages of fines but also the effect of environmental factors (rainfall, erosion, temperature, etc.) that can gradually reduce the characteristics of materials.

Table 3: Maximum density and optimum moisture content of materials

Materials	**Compaction characteristics**		**Carrying capacity characteristics**
	$W_{opt}(\%)$	$\gamma_{dmax}(kN/m^3)$	$CBR\ (\%)\ at\ 95\%\ of\ OPM$
Diack's basalt	4.2	22.05	86
Laterite of Sindia	9.66	19.7	54.8

Several rounds of CBR testing were conducted by [16] by first compacting the sample at its optimum moisture content and then at different Proctor curve moisture contents according to [11] conditions. The results show that the CBR obtained à 95% of the OPM of Diack basalt satisfies a base course. According to [17], the base course is subjected to significant stresses, the materials that constitute it must have sufficient qualities. However, the recommended CBR of 95% of the OPM must be at least 80%. The CBR of Sindia limestone can be used as a sub-base layer because it is higher than 30% [17].

In this three-dimensional modeling, a linear behavior is considered for the asphalt layer and subgrade with Young's moduli of 1300 MPa and 30 MPa respectively. The choice of the modulus for the wearing course is not arbitrary. [16] studied different types of pavements with moduli of 2300 MPa and 1300 MPa in the wearing course. The first modulus is not the usually used in Senegal. 1300 MPa represents the minimum modulus to avoid pavement failure [16]. It represents a reference modulus for a wearing course because the use of very high moduli leads to the use of low thicknesses and therefore to undersizing. The 2300 MPa modulus is obtained by iteration. Indeed, several moduli were tested starting with 1300 MPa. The gradual increase of this modulus up to 2200 MPa leads to a failure in the wearing course [16]. According to the researcher, the failure disappears once a value of 2300 MPa is reached for a flexible pavement with a base layer of untreated gravel and an 8 cm asphalt concrete wearing course. Hence the choice of a wearing course thickness of 8 cm throughout the modelling.

As for the base and sub-base layers, their behaviors are considered to be nonlinear. The reversible modulus is used to measure the nonlinear elastic properties for the granular materials constituting these layers. It is the modulus of elasticity of unbound materials based on elastic deformation from mechanical tests under cyclic loading. For a cyclic loading, the reversible modulus M_r of the material is defined by the following relation:

$$M_r = \frac{\Delta\sigma_d}{\Delta\varepsilon_1} \quad (1)$$

$\Delta\sigma_d = \sigma_1 - \sigma_3$ is the deviatoric stress;
σ_1 is the main major stress;
σ_3 is the minor stress;
$\Delta\varepsilon_1$ is the reversible axial strain.

Several models have been developed to determine the reversible modulus of granular materials as a function of state and stress level, thus allowing for the nonlinearity of these materials.

The $k-\theta$ model is most often used for the analysis of reversible behavior of granular materials and the study of the variation of stiffness with stress. [18] [19] [20] indicate that the reversible modulus is a function of the sum of principal stresses and propose a hyperbolic relationship commonly referred to as the $k-\theta$ model.

$$M_r = k_1 \left(\frac{\theta}{P_a}\right)^{k_2} \quad (2)$$

θ is the sum of the principal stresses (kPa);
k_1 and k_2 are the parameters of the model;
P_a is the atmospheric pressure of normalization.

Despite its simplicity in practice, this model has some shortcomings that have led some authors to make modifications.

A shortcoming of the $k-\theta$ model is related to the fact that the effect of stresses on the modulus is estimated only by the sum of the principal stresses. This model does not predict the volumetric strain and as such can only be applied if the confining stress is less than the deviatoric stress.

Since the $k-\theta$ model is not sufficient to describe the behavior of granular materials, [21] introduces a modification in the $k-\theta$ model. The introduction of deviatoric stress as an additional component with the consideration of the effect of shear behavior shows a good correlation with the test results.

$$M_r = k_1 \left(\frac{\theta}{P_a}\right)^{k_2} \left(\frac{\sigma_d}{P_a}\right)^{k_3} \quad (3)$$

θ is the sum of the principal stresses (kPa);
σ_d is the deviatoric stress;
k_1, k_2 and k_3 are the parameters of the model;

Uzan's model seems to be in accordance with all aspects that characterize the behavior of granular materials. By considering the sum of stresses and the deviatoric stress, Uzan's model takes into account the shortcomings of the $k-\theta$ model which does not include the effects of shear and therefore better matches the experimental results. This problem was especially emphasized when the values of confining stresses applied on the sample were higher than the deviatoric stresses applied during the test.

A generalized model is proposed by NCHRP Project 1-28A (2004) to characterize the reversible modulus of untreated gravel and fine soils. This equation (4) combines the hardening effect of the sum of the principal stresses and the softening effect of the shear stress.

$$M_r = k_1 . P_a \left(\frac{\theta}{P_a}\right)^{k_2} \left(\frac{\tau_{oct}}{P_a} + 1\right)^{k_3} \quad (4)$$

θ is the sum of the principal stresses (kPa);
τ_{oct} is the octahedral shear stress
k_1, k_2 and k_3 are the parameters of the model

$$\tau_{oct} = \frac{1}{3}\sqrt{(\sigma_1 - \sigma_2)^2 + (\sigma_2 - \sigma_3)^2 + (\sigma_3 - \sigma_1)^2} \quad (5)$$

In the finite element modeling, which is the focus of this paper, only the parameters k_i of the different models ($k-\theta$, Uzan, NCHRP) will be used. Triaxial repeated loading tests for the study of reversible behavior were performed by [11] on Diack basalt at the University of Wisconsin and those of Sindia laterite are being performed by [10] at IFSTTAR in Nantes.

The determination of the parameters k_i of the models ($k-\theta$, Uzan, NCHRP) is done from the regression of the results of cyclic triaxle tests. The chosen fitting method, based on the least squares method, is inexpensive in time and allows a large number of calculations.

For all the adjustments, we used an option (solver) of the Excel spreadsheet, allowing, on the basis of the method of least squares, to seek the set of parameters which minimizes the differences between the experimentally measured values calculated by the model. The different parameters k_i of the different models are summarized in table 4.

Table 4: Values k_i of the different models

		k-Ɵ		Uzan			NCHRP		
Material	**w_{opt} (%)**	**k_1 (MPa)**	**k_2**	**k_1 (MPa)**	**k_2**	**k_3**	**k_1 (MPa)**	**k_2**	**k_3**
Diack's basalt	4.2	147	0.53	93717	1	-0.32	1224	0.93	-0.52
Laterite of Sindia	9.66	121	0.20	837	0,13	-0.33	113	0.07	-0.62

To determine the Young's moduli E of base and sub-base materials, the nonlinear elasticity model $k-\theta$ was calibrated on the results of these tests to determine the parameters k_1 et k_2. These parameters allow the calculation of a reference value of the Young's modulus according to the NF P 98-235-1 standard (q= 600 kPa, P= 300kPa). The different moduli obtained as a function of the optimum water content are summarized in table 5.

Table 5: Young's modulus values

Material	**Content of Optimal water w_{opt} (%)**	**Young's modulus E_c (MPa)**
Diack's basalt	4.2	139
Laterite of Sindia	9.66	118

Preliminary simulations

The preliminary simulations presented here are carried out in order to optimize the numerical simulations to the undertaken in the following. Indeed, the more the model studied is discretized, the longer the simulations time is. These numerical simulations concern a pavement structure consisting of a wearing course in asphalt concrete, a base course consisting of Diack basalt, a sub-base course consisting of Sindia laterite and a support soil. It is then necessary to check beforehand that the dimensions of the model, the mesh level of the structure and the chosen boundary conditions allow to optimize the computation time of the solution while preserving the quality of the model response.

Optimization of the domain geometry

In order to verify the sensitivity of the measurements, several dimensions of the domain were tested. For this purpose, simulations were performed to evaluate the impact of varying the mesh size and domain boundaries on the accuracy of the results. For these tests, the mesh size of the pavement structure must be chosen so that the pavement response is not influenced by this parameter.

$\alpha R * \beta R = pavement\ length\ * pavement\ width$

$\alpha = \beta = 10\ ;\ 20\ ;\ 30\ ;\ 40$

R is the radius of the circular footprint of the wheel;

γ is the optimal thickness of the platform to find.

Table 6: Materials parameters

Layers	**Nature of the layers**	**Thickness (m)**	**Density (kg/m^3)**	**E(MPa)**	**Poisson's ratio ν**
Surface	Asphalt concrete	0.08	-	1300	0.35
Base	Diack's basalt	0.25	2417	139	0.35
Sub-base	Laterite of Sindia	0.25	1970	118	0.35
Subgrade	-	γ	-	30	0.35

Figures 3, 4 and 5 illustrate the evolution of strains and stresses on particular points of the structure as a function of pavement depth. By choosing a tolerance of 5% of relative error on the results, the total depth retained for the

pavement is 2,5 m, that's to say 20R. In the nonlinear modelling, a pavement structure of width 30R, length 30R and depth 3 m (24R) will be considered.

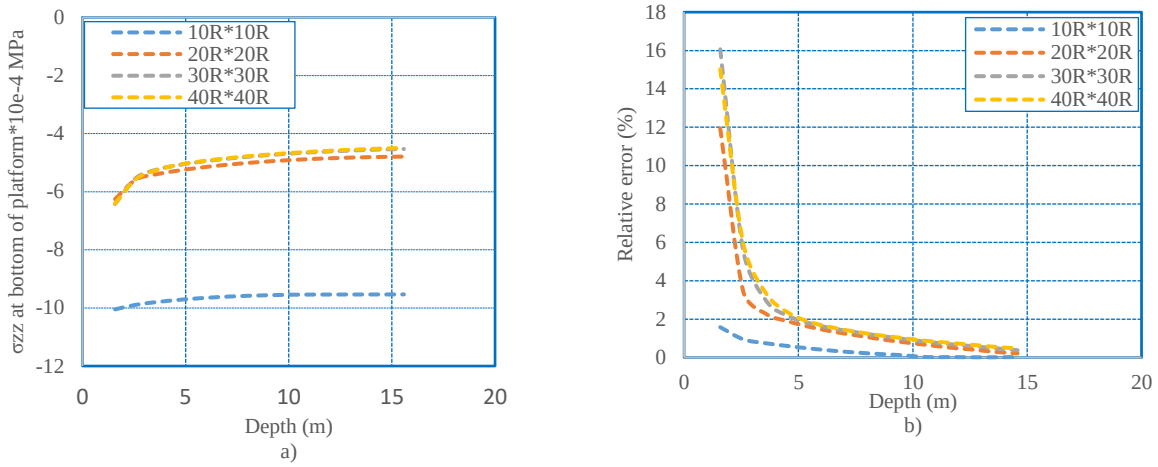

Figure 3: Effect of geometry variation: a) vertical stress at bottom of subgrade; b) relative error

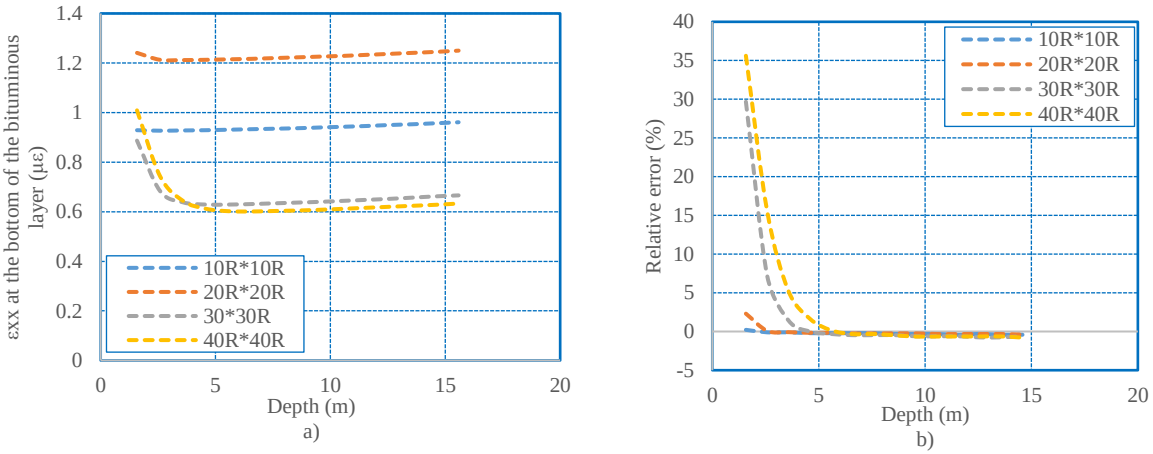

Figure 4: Effect of geometry variation: a) radial strain; b) relative error

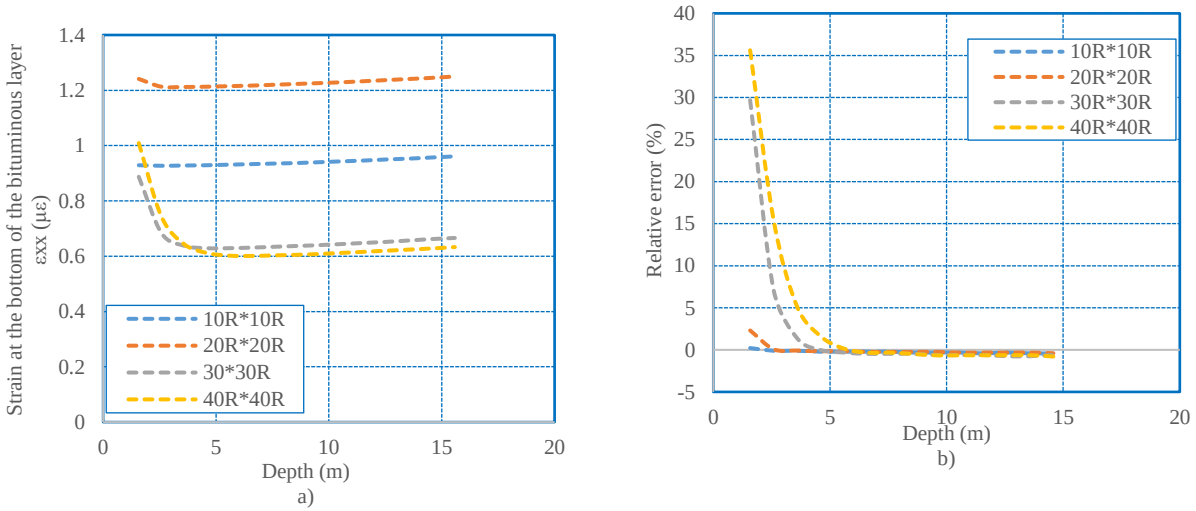

Figure 5: Effect of geometry variation: a) radial strain; b) relative error

Effect of mesh sensitivity

To study the mesh sensitivity, 14 mesh types were considered and the vertical strains over the different layers of the structure are calculated. Figure 6 shows the variations of these strains as a function of the total number of CUB8 elements in the structure. These strains stabilize from 11200 elements. In order words, the response of the pavement is slightly modified from this value. In the rest of the modelling, this value will be considered.

Table 7: Different meshes tested

Mesh	Number of elements CUB8	Mesh	Number of elements CUB8
M1	2400	M8	8000
M2	3200	M9	9600
M3	4000	M10	11200
M4	4800	M11	12000
M5	5600	M12	16000
M6	6000	M13	20000
M7	6400	M14	24000

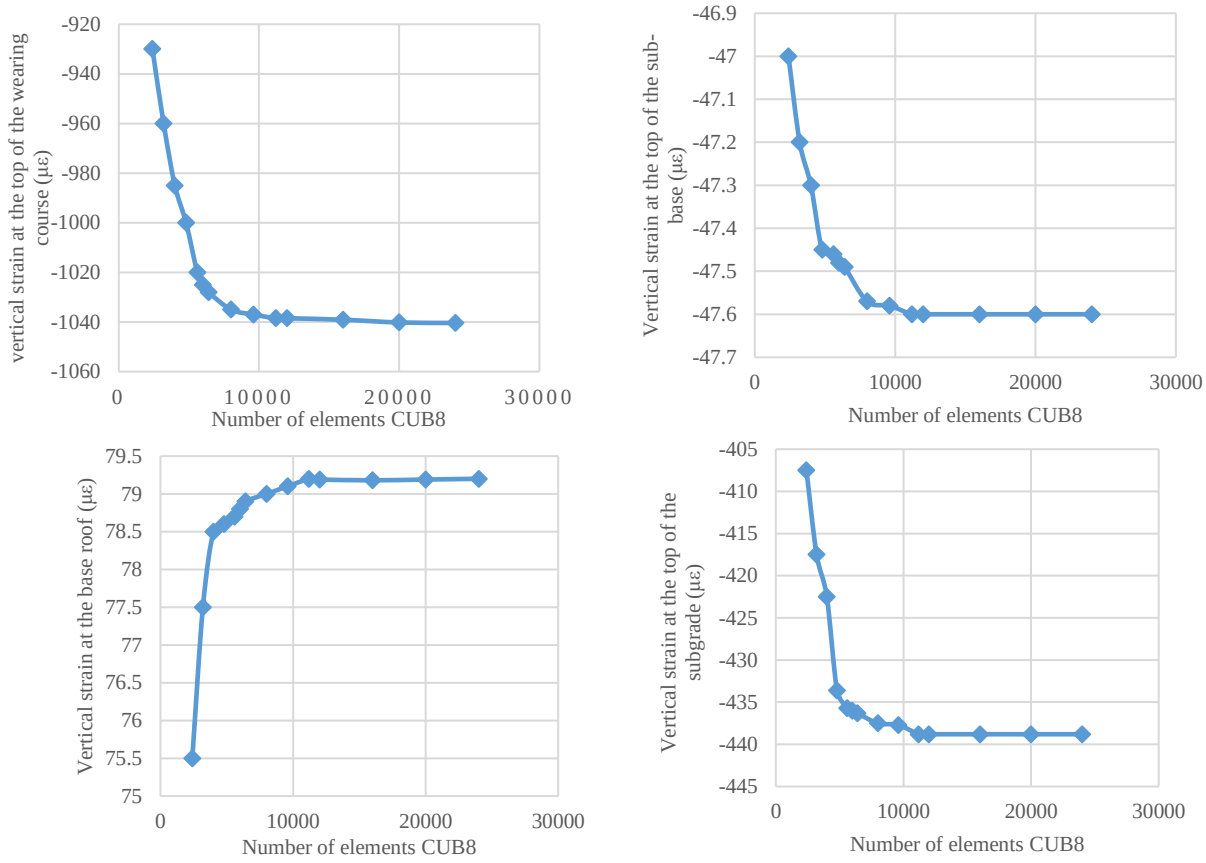

Figure 6: Curves illustrating the sensitivity of the mesh quality to the number of element in the structure

Influence of the loading pitch

The results show that the loading step has an impact on the vertical strain at the top of the pavement layers. However, this strain seems to stabilize when the number of loading steps reaches 50. In the rest of the modelling, this number of loading steps is considered.

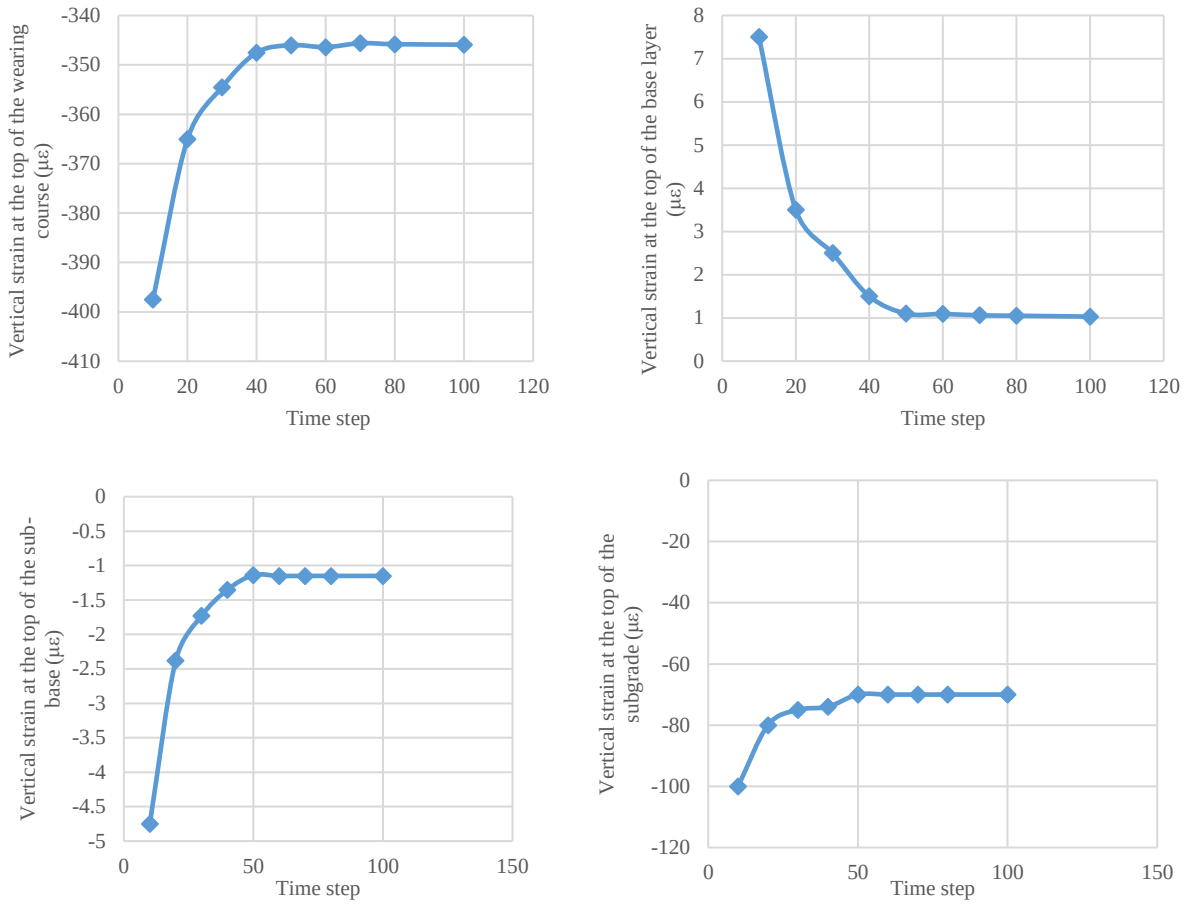

Figure 7: Curves illustrating the influence of the loading step on the vertical strain at the top of the pavement layers

The implementation of the Uzan model and those of the $k-\theta$ and NCHRP models is used for pavement base modeling by integrating the model parameters into the tangent stiffness matrix equation. In equation 6, the parameters of the Uzan model are incorporated.

$$D_T = \left[\frac{-k_2\left(\frac{\theta+\theta_t}{P_a}\right)^{-k_2-1}\left(\frac{\sigma_d}{P_a}\right)^{-k_3}}{k_1{P_a}^2} + \frac{-k_3\frac{15\sqrt{2}}{3}\left(\frac{\theta+\theta_t}{P_a}\right)^{k_3}\left(\frac{\sigma_d}{P_a}\right)^{-k_3-1}}{k_1{P_a}^2}\right]\sigma_1 + \left[\frac{\left(\frac{\theta+\theta_t}{P_a}\right)^{-k_3}\left(\frac{\sigma_d}{P_a}\right)^{-k_3}}{k_1 P_a}\right] \quad (6)$$

θ is the sum of the main constraints;
σ_d is the deviatoric stress;
P_a is the atmospheric pressure of normalization.
Figure 8 shows the computational algorithm used for the implementation of the different models.

The nonlinear analysis consists of several iterations. A linear analysis is performed in each iteration, after which the reversible modulus of each finite element is improved as needed. The iteration is repeated until the reversible moduli of all elements stabilize.
An iterative macro is created, the material properties change at each iteration, in relation to the stress state of each element, until arriving at the convergence criterion as for example the one of [22] presented in equation (7).

$$\frac{\sum_{i=1}^{n}|E_{newi}-E_{oldi}|}{\sum_{i=1}^{n}E_{oldi}} \times 100 \leq 5 \quad (7)$$

n, number of elements in the layer
E_{newi}, modulus of element i for the iteration
E_{oldi} , modulus of the element i for the previous iteration

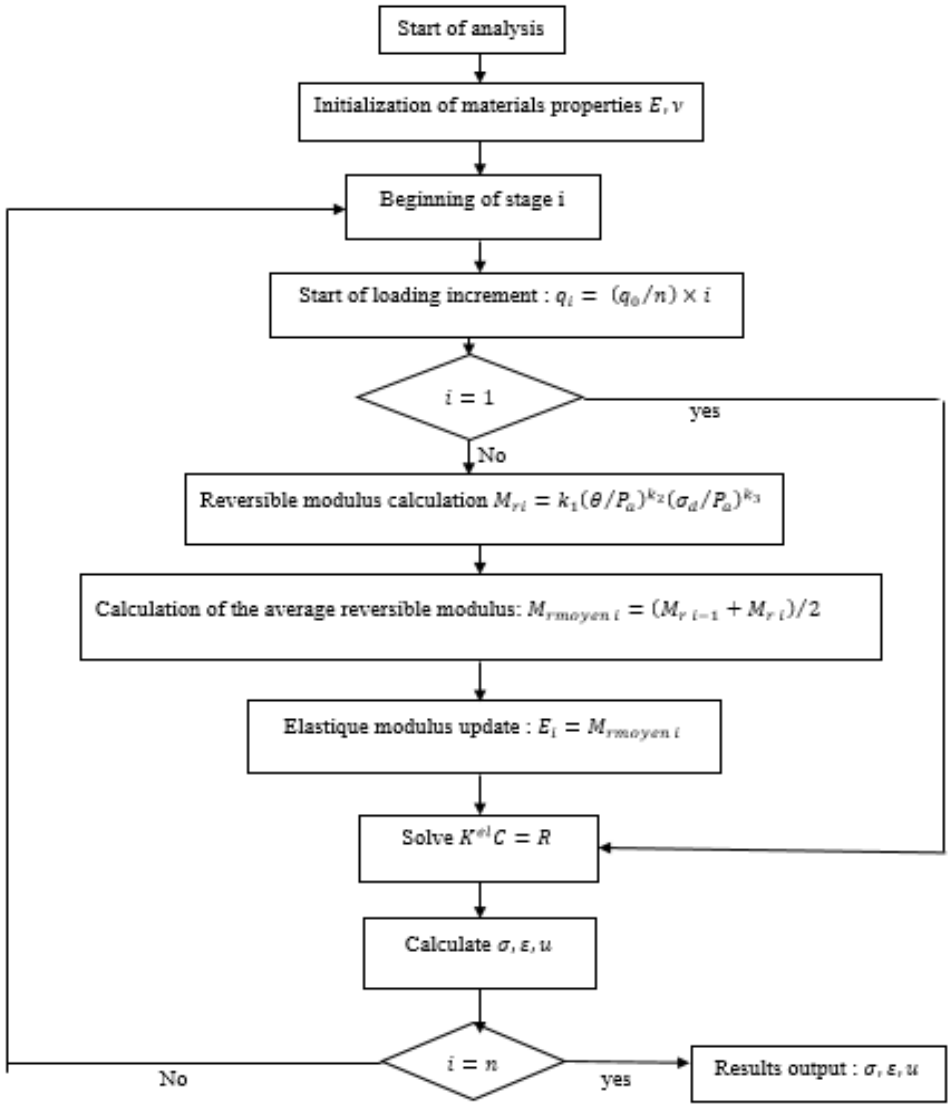

Figure 8: Flow chart of the nonlinear analysis [3]

Impact of axle configuration

Given the technology of the vehicles, it can be noted that the latter has significant consequences on the degradation of the pavements. An attempt at finite element modeling under Cast3M is then considered to study the effect of the axle configuration on the pavement.

Modeling of the pavement structure

The base of the pavement structure considered is made of unbound granular materials. The base course is made of Diack basalt, the sub-base of Sindia laterite, the wearing course of asphalt concrete and the whole structure rests on a support subgrade. To study the impact of not taking into account the nonlinearity in the design of pavements in Senegal, a first structure with a base made of materials with a supposedly linear behavior will be studied. As for the other structure, the base is made of the same materials but with nonlinear behavior. The $k-\theta$, Uzan and NCHRP models will be studied to Investigate the nonlinear behavior of the said materials. Stresses and strains are calculated for loading with a single wheel and with a dual wheel in order to compare the results obtained with the two types of loading.

For the study of the effect of axle configuration (single or dual wheel), the input parameters used are those of the linear (table 8) and nonlinear models (tables 9, 10 and 11). In the further modeling of the structure, the nonlinear models used are the $k-\theta$, Uzan and NCHRP models.

Results and Interpretations

It is generally found that stresses and strains decrease with depth. This could be explained by the decrease in the distribution of stresses at depth, also generating low strains. This difference in responses is confirmed by the literature [5] [6] [7].

It is also noted that the stresses and strains created by the single wheel are greater than that of the dual wheel at the surface of the wearing course. However, at a certain depth of this layer, there is an inversion, the stresses and strains created by the dual wheels are greater up the base of the base layer.

It can be seen that this difference decreases very quickly in the sub-base and even tends to cancel out in some cases up to the subgrade. It could be concluded that for the considered pavement structure, the difference of the stresses and strains caused by the axle configuration (single or dual wheels) is more important until the base of the base layer, but it tends to decrease from the sub-base layer. All these results are illustrated in the figures 9, 10 and 11.

Table 8: Material parameters (linear model)

Layer	Nature des Couches	Thickness (m)	Density (kg/m^3)	E(MPa)	Poisson ratio ν
Surface	Asphalt concrete	0,08	-	1300	0,35
Base	Diack's basalt	0,25	2417	139	0,35
Sub-base	Laterite of Sindia	0,25	2020	118	0,35
Subgrade	-	2,42	-	30	0,35

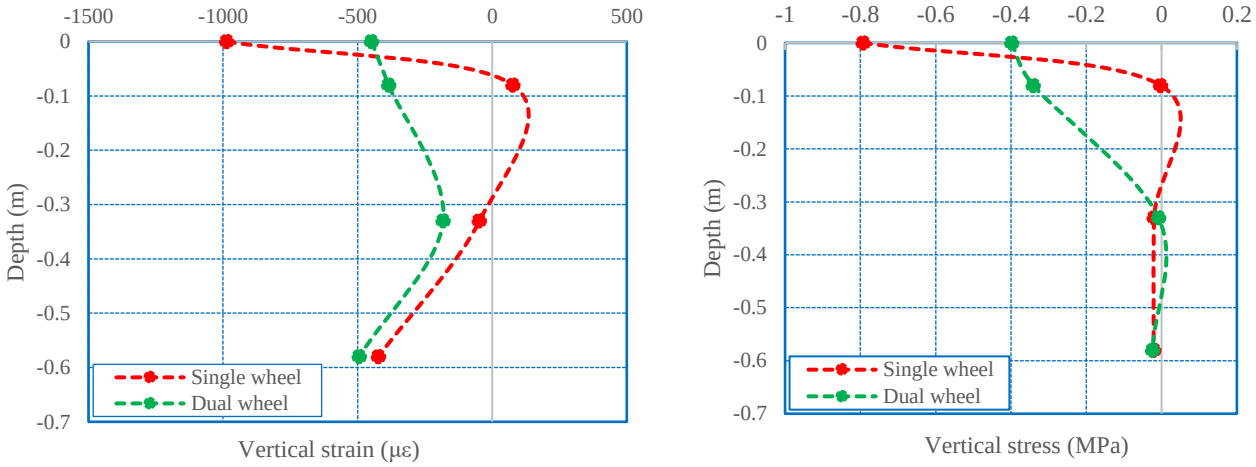

Figure 9: Variation of vertical strain and stress with depth (linear model)

Table 9: Model parameters $k-\theta$

Layers	Nature of layer	Thickness (mm)	Linear model		Nonlinear model	
		$e_i\ (m)$	υ	$E(MPa)$	$k_1(MPa)$	k_2
Surface	AC	0.08	0.35	1300	-	-
Base	BD	0.25	0.35	-	147	0.53
Sub-base	LS	0.25	0.35	-	229	0.49
Subgrade	-	2.42	0.35	30	-	-

AC: Asphalt concrete BS: Diack's basalt LS: Laterite of Sindia

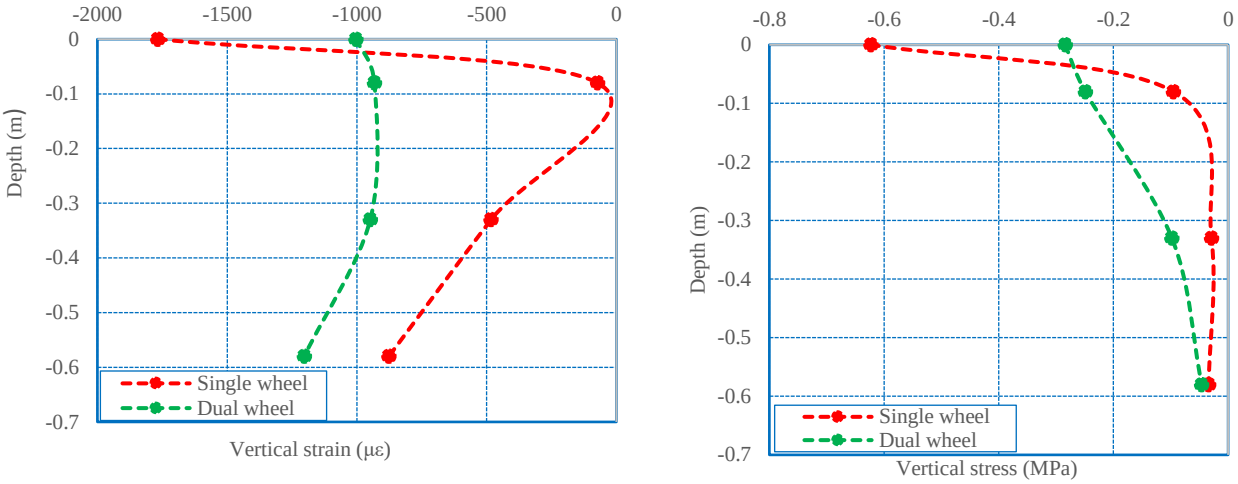

Figure 10: Variation of vertical strain and stress with depth $(k-\theta)$

Table 10: Parameters of the Uzan model

Layers	Nature of the layers	Thickness (mm)	Linear model		Nonlinear model		
		$e_i\,(m)$	υ	$E(MPa)$	$k_1(MPa)$	k_2	k_3
Surface	AC	0,08	0,35	1300	-	-	-
Base	BD	0,25	0,25	-	93717	1,00	- 0,32
Sub-base	LS	0,25	0,25	-	133017	1,05	-0,53
Subgrade	-	2,42	0,25	30	-	-	-

AC: Asphalt concrete BS: Diack's basalt LS: Laterite of Sindia

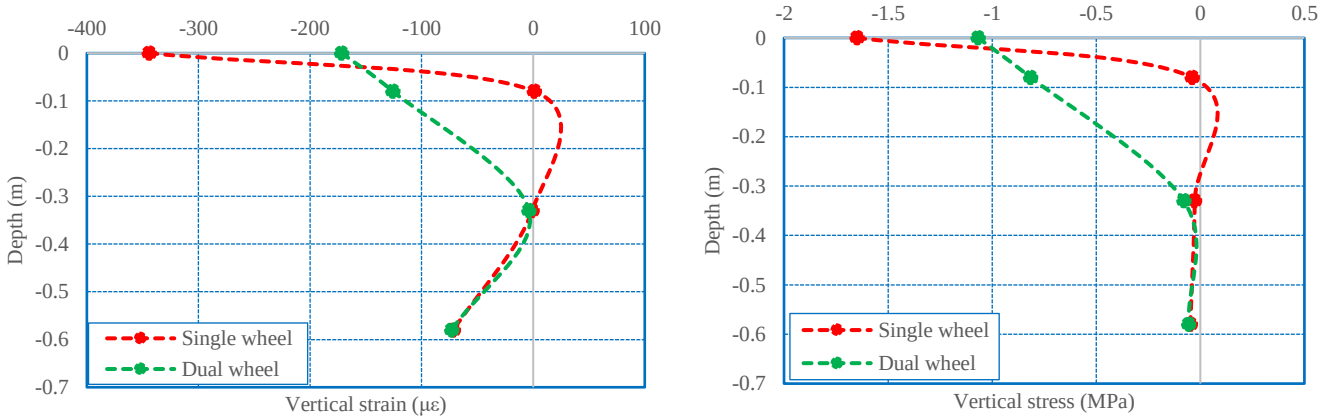

Figure 11: Variation of vertical strain and stress with depth (Uzan)

Table 11 : NCHRP model parameters

Layers	Nature of the layers	Thickness (mm)	Linear model		Nonlinear model		
		$e_i\,(m)$	υ	$E(MPa)$	$k_1(MPa)$	k_2	k_3
Surface	AC	0.08	0.35	1300	-	-	-
Base	BD	0.25	0.35	-	1224	0.93	- 0.52
Sub-base	LS	0.25	0.35	-	2097	0.98	-0.96
Subgrade	-	2.42	0.35	30	-	-	-

AC: Asphalt concrete BS: Diack's basalt LS: Laterite of Sindia

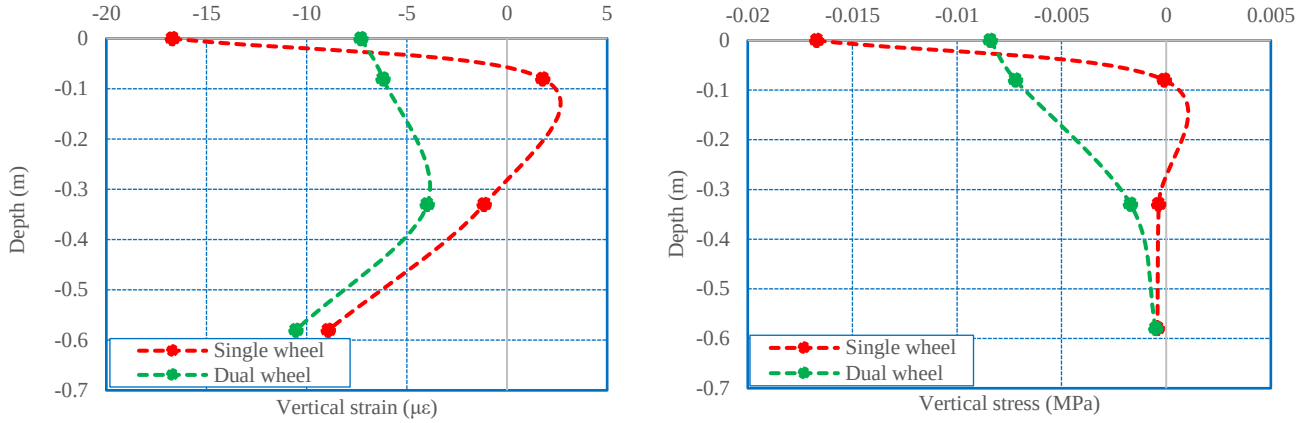

Figure 12: Variation of vertical strain and stress with depth (NCHRP)

Distribution of vertical contact stress

The vertical contact stress distribution is studied by considering two types of loading of a 65 kN half axle. For a single wheel loading, the entire load is applied. For a dual wheel loading, the load is distributed over two circular areas. The vertical strain is measured on three points of the circular area, as illustrated in figure 13.

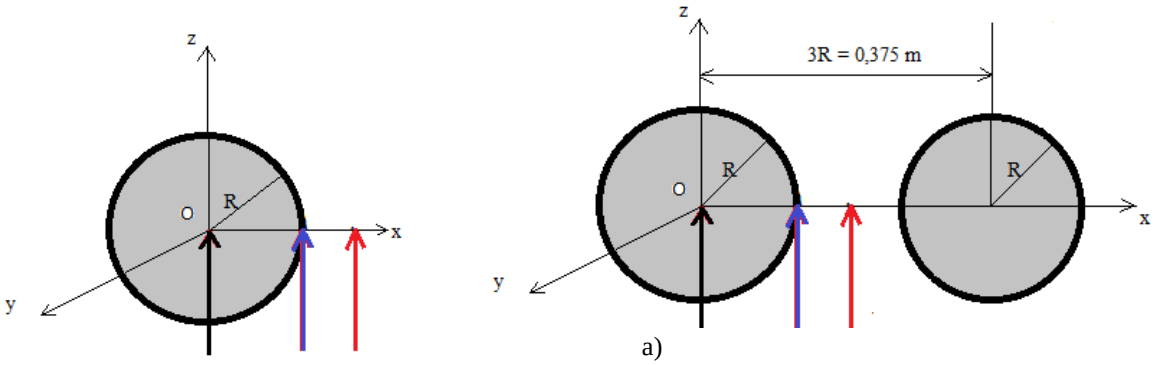

Figure 13: Loading diagram: a) single wheel b) dual wheels

The evolution of the vertical strain on different points will be studied. The characteristics of the materials constituting the structure are summarized in table 12.

Table 12: Parameters of the materials constituting the considered structures

Pavement layers	Thickness (mm)	Linear model		Nonlinear model				
				k-Θ		Uzan		
	$e_i\ (m)$	ν	$E(MPa)$	$k_1(MPa)$	k_2	$k_1(MPa)$	k_2	k_3
Surface (AC)	0,08	0,35	1300	-	-	-	-	-
Base (BAS)	0,25	0,35	-	147	0,53	1224	0,93	- 0,52
Sub-base (LS)	0,25	0,35	-	229	0,49	2097	0,98	-0,96
Subgrade	2,42	0,35	30	-	-	-	-	-

AC: Asphalt concrete BS: Diack's basalt LS: Laterite of Sindia

The results show, for the pavement layers, that the strains obtained at the center is greater than those obtained at the edge of the footprint and in the middle of the axle (figure 14, figure 15).

It is also generally observed that the evolution of the vertical strain at the footprint is almost the same at the level of the base layer, the sub-base and the subgrade. However, the largest differences are noted at the level of the asphalt layer.

To illustrate the difference in strain that exists between the different positions of the cavity (edge and middle) in relation to the center of the cavity, taken arbitrarily as a reference, we determined the relative error according to the formula below:

$$Relative\ error\ (\%) = \frac{Strain\ (center) - strain\ (edge/middle)}{strain\ (edge/middle)} \times 100 \quad (8)$$

The vertical strains obtained with the $k-\theta$ and Uzan models are illustrated in the figures 14 and 15. As for the relative errors, they are summarized in tables 13 and 14.

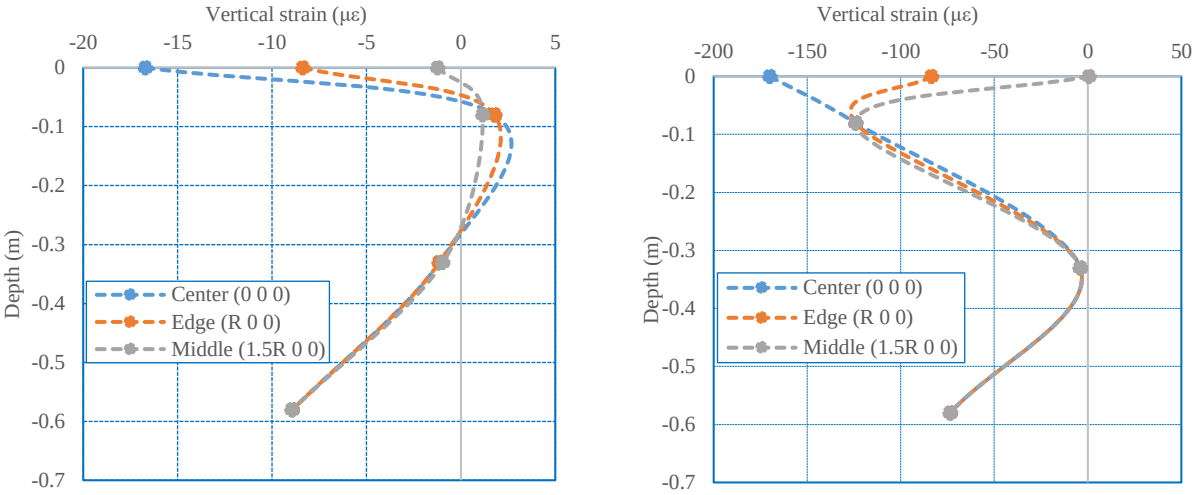

Figure 14: Evolution of the vertical strain in the structure (Uzan model): a) single wheel b) dual wheels

Table 13: Relative error on vertical strain above the layers of the structure (Uzan)

Root of the layer of :	Relative error (%)			
	Single wheel		Dual wheel	
	edge	middle	edge	middle
Bearing	100	1262	103	28633
Base	0	54	0	0
Sub-base	0	20	0	0
Subgrade	0	0	0	0

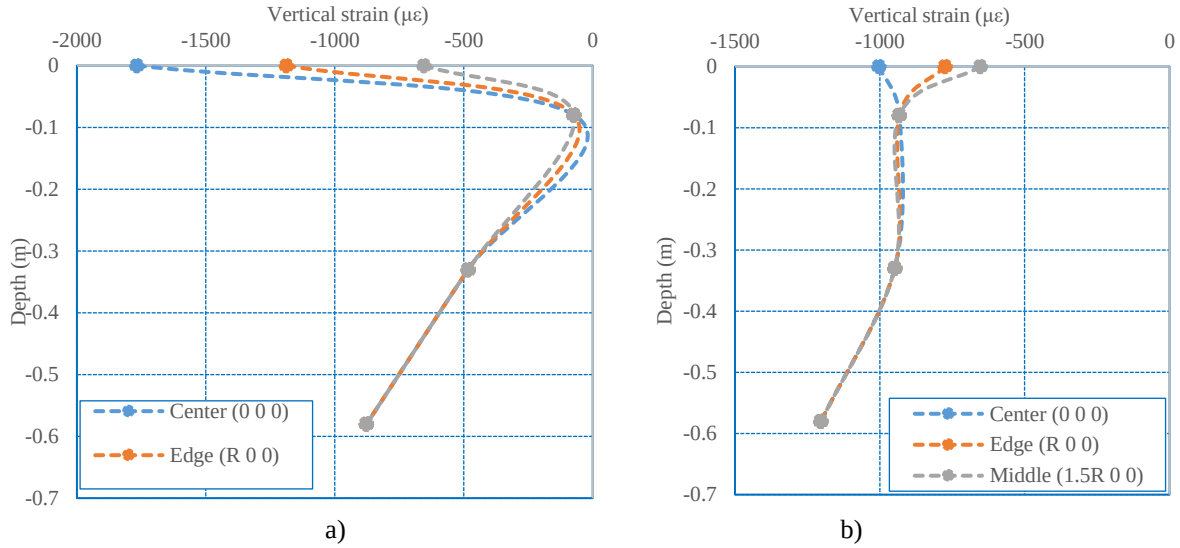

Figure 15: Evolution of vertical strain in the structure (model $k-\theta$) : a) single wheel b) dual wheel

Table 14: Relative error on vertical strain over the layers of the structure $(k-\theta)$.

Root of the layer of:	Relative error (%)			
	Single wheel		Dual wheel	
	edge	middle	edge	middle
Bearing	49	170	30	54
Base	0	0	0	0
Sub-base	0	0	0	0
Subgrade	0	0	0	0

In the end, the results show that with all the studied loadings and the different models used, it can be concluded that the vertical strain is no uniform on the circular footprint and has a significant influence on the strain of the asphalt wearing course. The strain is maximum in the center of the circular footprint. However, this vertical contact stress distribution has no influence from the base layer to the subgrade layer. These results show that no uniform distributions of vertical contact stress can be studied in the model.

Conclusion

pavement structure, that's to say to understand the variation of the stress and strain state in the pavement structure during the passage of traffic loads. Traffic is the most important parameter in pavement design. The stresses taken into account in road design are derived from traffic loads. The determination of these loads in the pavement is performed by numerical simulation with the finite element code Cast3M. For the considered pavement structure, the base and sub-base layers all have a nonlinear behavior, a simulation is performed with the implementation of $(k-\theta)$, Uzan and NCHRP models in the Cast3M software.

Before starting the numerical simulation, a preliminary study is made on the optimal choice of the domain geometry, the number of CUB8 elements and the loading time step. A pavement structure of width 30R, length 30R and depth 3m (24R) is chosen and a number of CUB8 elements equal to 11200 with a loading step taken equal to 50.

The analysis of the results obtained generally shows that the damage caused by the single wheel is higher than that of the dual wheel at the surface of the wearing course. However, there is a reversal of this damage at a certain depth of the wearing course, that's to say the damage caused by the dual wheel is greater up to the base of the base course. It can be seen that this difference decreases very quickly in the sub-base layer and even tends to cancel out in some cases down to the subgrade. The vertical strain difference caused by the type of loading increases as one approaches the subgrade. The difference in damage caused by the axle configuration (single or dual wheel) seems to be greater up to the base of the base layer, but tends to decrease from the sub-base layer.

The results also showed in general that the evolution of the vertical strain at the footprint is almost the same at the level of the base layer, sub-base and subgrade. However, the maximum deviations are most important at the level of the asphalt layer.

This information could be used to improve the design of pavement structures with respect to axle configuration, to study in the modeling no uniform distributions of vertical contact stress and even to review the shape of the loading footprint which is assumed circular in the design.

References

[1]. Kim, Y.R. (2010). « Impact of truck loading on design and analysis of asphaltic pavement structures », Department of civil Engineering University of Nebraska-Lincoln, p. 55.

[2]. Gidel, G. (2001). « Comportement et valorisation des graves non traitées calcaires utilisées pour les assises de chaussées souples » Thèse de doctorat, Université de Bordeaux I, 32-55.

[3]. Samb, F. (2014). « Modélisation par éléments finis des chaussées en graveleux latéritiques traités ou non et application au dimensionnement Mécanistique – Empirique » Thèse de doctorat, Université de Thiès, 88-113.

[4]. Zienkiewicz, O. C., &Taylor, R. (1989). « The finite element method », Vol. 1: Basic concepts and linear application, 4e édition, Mc Graw-Hill, London, p. 233.

[5]. Gillespie, D., Karanuhao, M., Sayers, W., Nasim, A., Hasen, W., & Cabon, D. (1993). « Effects of heavy – Vehicle caracteristic on pavement responses and performance » NCHRP Report 353. National Cooperative Highway Research Program, Transportation Research Board. Washington, p.132.

[6]. Stolarski, H. (1999). « Load testing of instrument pavement section », University of Minnesota Department of Civil Engineering submitted to: M_n/DOT Office of Materials and Road Research Maplewood, P.23.
[7]. Perret J., & Dumont A., G. (2004). « High modulus pavement design using accelerated loading testing », 3rd Eurasphalt and Eurobitume Congess Vienna, p. 10.
[8]. Roberto, F.S. (2005). « Finite element analysis of the mechanics of viscoelastic asphaltic pavements subjected to varying tire configurations » PhD thesis, Nebraska University, p.16.
[9]. Akram, T., Scullion, T., Smith, R. E., & Fernando, E.G. (1992). « Estimating damage effects of dual versus wide base tires with multidepth deflectometers », Transportation Research Record 1355, p. 60.
[10]. Sebaaly, P., & Tabatabee, N. (1989). « Models for damage growth and fracture in nonlinear viscoelastic particulate composites », proceeding of the 9th U.S. National Congress of Applied Mechanics, Applied Mechanics Reviews, 57, 269-275.
[11]. Ba, M. (2012). « Comportement mécaniques sous sollicitations cycliques de granulats quartzitiques de Bakel – Comparaison avec des matériaux de référence du Sénégal et d'Amérique (USA). Application au dimensionnement mécanistique – empirique des chaussées souples » Thèse de doctorat, Université Cheikh Anta Diop de Dakar, 53-74.
[12]. Ki, B.I.J. (2021). « Effect of water content and gain size distribution on the characteristic resilient Young's modulus obtained using anisotropic Boyce model on gravelly lateritic soils from tropical Africa (Burkina Faso and Senegal), 137-141.
[13]. CEBTP (1984). « Guide Pratique de dimensionnement dans les pays tropicaux » Ministère français de la coopération, p.77.
[14]. Ndiaye, M. (2013). « Contribution à l'étude de sols latéritiques du Sénégal et du Brésil » Thèse de doctorat, Université Paris-Est et Université Cheikh Anta Diop de Dakar, p.50.
[15]. Bérubé, M. A. (2001). « Aggregate technology. Notes from the course LG-18832; Aggregate technology, Department of Geology and Geological Engineering, Laval University, Quebec, p.17.
[16]. Dione, A. (2014). « Estimation du module réversible de graves non traitées et modélisation par éléments finis de chaussées souples en vue d'un dimensionnement mécanistique-empirique » Thèse de doctorat, Université de Thiès, 56-97.
[17]. CEBTP (1984). « Guide Pratique de dimensionnement dans les pays tropicaux » Ministère français de la coopération, p.77.
[18]. Seed, H. B., Mitry, F. G., Monismith, C. L., & Chan, C. K. (1965). « Predictions of pavement deflection from laboratory repeated load tests », Rep. N°. TE-65-6, Soil Mech. And Bituminous Mat. Res. Lab., University of California, Berkely, Berkeley, Calif, p.36.
[19]. Brown, S. F., & Pell, P. S. (1967). **«** An experimental investigation of the stresses, strains and deflections in a layered pavement structure subjected to dynamic loads », Proc., 2nd Int. Conf. Struct. Des. of Asphalt Pavements, 487-504.
[20]. Hicks, R.G. (1970). « Factors influencing the resilient properties of granular materials ». PhD thesis, University of California, Berkeley, Berkeley, Calif, p.30.
[21]. Uzan, J. (1985). « Characterization of granular material ». Transp. Res. Rec. 1022, Transportation Research Board, Washington, D.C., 52-59.
[22]. Le Vern, M. (2016). « Conception mécaniste-empirique des chaussées non revêtues », Université Laval, p.32.